ROTOR AEROELASTIC STABILITY COUPLED WITH HELICOPTER BODY MOTION

Wen-Liu Miao
Boeing Vertol Company
Philadelphia, Pennsylvania

Helmut B. Huber
Messerschmitt-Boelkow-Blohm Gmbh
Ottobrun-Munich
Federal Republic of Germany

Abstract

A 5.5-foot-diameter, soft-in-plane, hingeless-rotor system was tested on a gimbal which allowed the helicopter rigid-body pitch and roll motions. With this model, coupled rotor/airframe aeroelastic stability boundaries were explored and the modal damping ratios were measured. The time histories were correlated with analysis with excellent agreement.

The effects of forward speed and some rotor design parameters on the coupled rotor/airframe stability were explored both by model and analysis. Some physical insights into the coupled stability phenomenon were suggested.

Introduction

The coupled rotor-airframe aeroelastic stability phenomenon of air resonance has received considerable attention in recent years. A scaled model of the BO-105 helicopter was built and tested to explore this phenomenon and its sensitivity to design parameters.[1] An extensive analytical study was performed and correlated with BO-105 flight test data.[2]

To further explore this coupled stability phenomenon, a large scale model having different resonance characteristics than the BO-105 was built and tested. Parameters that were influential to the stability[1, 2] were incorporated into the model and their effects were examined. An improved test technique enabled the determination of modal damping ratio at every test point, providing better data for correlation and better assessment of stability.

Description of Model

The model, shown in Figure 1, consisted of a Froude-scaled model rotor mounted on a rigid fuselage, which in turn was mounted on a two-axis gimbal having ± 10 degrees travel in pitch and roll. The model had a 5.5-foot-diameter, soft-in-plane, hingeless rotor with pertinent hub parameters such as precone, sweep, and control system stiffness being variables to enable investigation of their effects on coupled rotor-airframe stability.

A proportional (closed-loop) control system equipped with a cyclic stick provided lateral and longitudinal control to fly the model in the pitch and roll degrees of freedom. In addition, a shaker system was installed in the longitudinal and lateral cyclic system

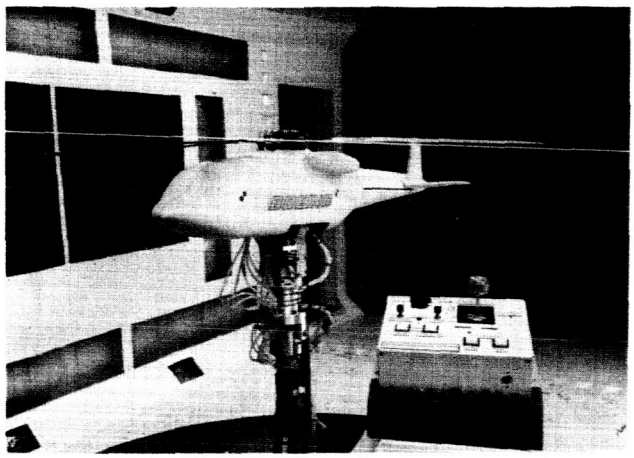

Figure 1. Dynamic Model Helicopter With 5.5-Foot-Diameter Single Rotor

(see Figure 2) to allow excitation of the model at the desired frequency. This enabled the measurement of the modal damping ratios at each test point. The measured modal damping permitted the precise determination of the stability boundaries and also showed the extent of stability when the model was stable.

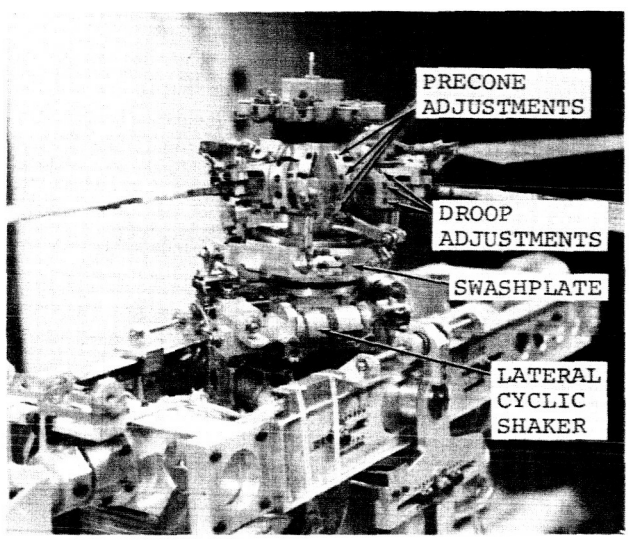

Figure 2. Details of Model Rotor Hub and Swashplate

Presented at the AHS/NASA-Ames Specialists Meeting on Rotorcraft Dynamics, February 13-15, 1974.

The stability and control augmentation system was based on position feedback. Position potentiometers on the helicopter gimbal axes provided position feedback signals which were amplified, filtered, and fed into the cyclic actuators for automatic stabilization of the model. The filter was designed to block any feedback at a frequency of $\Omega-\omega_\zeta$ and thus eliminated any control inputs that would tend to interact with the air-resonance mode.

Collective pitch was set by means of an open-loop control and a pitch-angle indicator. Other controls provided for the operator included mounting-pylon pitch attitude, stick trim, and quick-acting and slow-acting, self-centering snubbers to lock out the pitch and roll degrees of freedom. The horizontal stabilizer was manually trimmable and rotor speed was controlled by the wind tunnel operator.

Signals from the blade flap, torsion, and chord strain gages, along with body pitch and roll motion, cyclic stick position, and 1/rev, were recorded on oscillograph as well as on multiplex tape recorder. One of the chord-bending traces was filtered to display the chord bending at the critical lag natural frequency to allow quick determination of modal damping on line. Most of the testing was performed in the wind tunnel at the University of Maryland.

Test Technique

As discussed in References 1 and 2, the air-resonance mode stability is determined by the blade collective pitch as well as the rotor speed. Therefore, for every airspeed, a comprehensive variation of rpm and collective pitch was conducted.

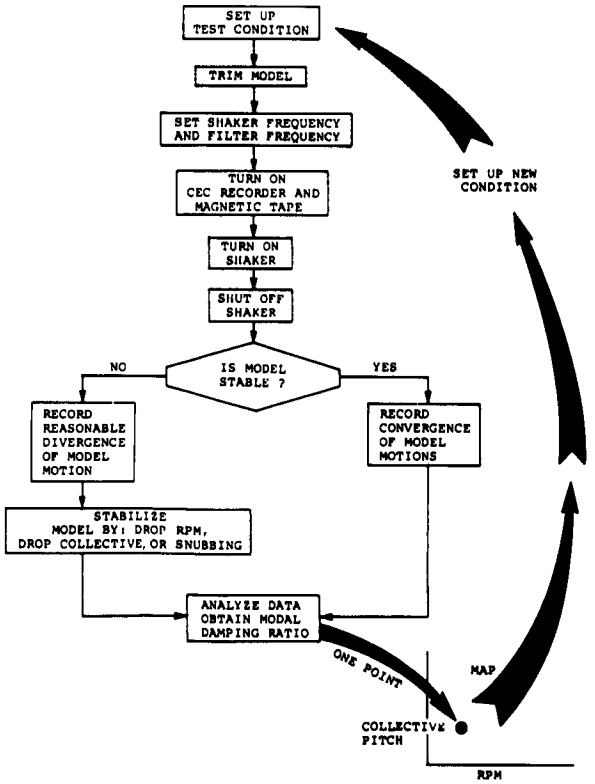

Figure 3. Flow Diagram of Test Technique

Figure 3 shows the test flow of events for each data point taken. After the test conditions had been set up (rpm, tunnel speed, and collective pitch), the model was trimmed and was held at the trim attitude with the stability and control augmentation system (SCAS). The shaker and the tracking filter frequencies were set to $\Omega-\omega_\zeta$ and ω_ζ respectively, with the absolute magnitudes dependent on the rotor speed. Both the multiplex tape recorder and the CEC recorders were turned on to record the steady-state response of the model. The swashplate was then oscillated in the lateral control direction. After the termination of the excitation, recording was continued until steady-state conditions were again reached, when practical. The decay of the filtered, in-plane, bending-moment trace was reduced to obtain the modal damping ratio.

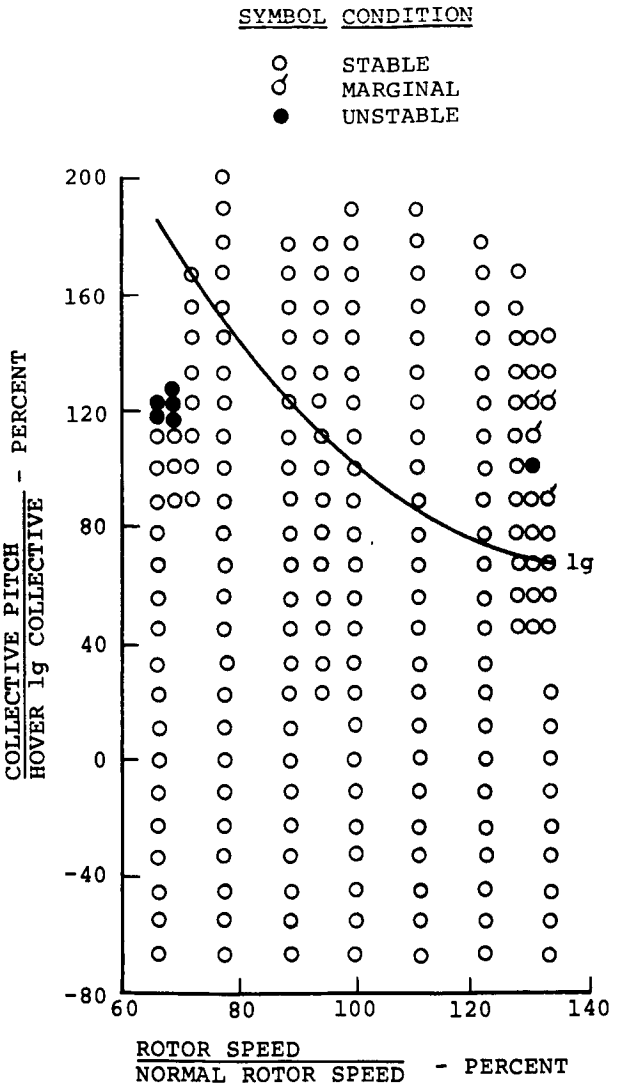

Figure 4. Typical Map of Test Points in Hover

Test Results

Figure 4 shows a typical map of test points taken at a constant tunnel speed, in this case in hover. Two

stability boundaries were present: one at about 70 percent of normal rotor speed and 120 percent of normal collective pitch and another at about 135 percent rpm and 100 percent collective. Examination of the coupled frequency variation with rotor speed while holding constant thrust, Figure 5, reveals that the low-rpm boundary corresponds to the resonance with the body-pitch-predominant mode and the high-rpm boundary with the body-roll-predominant mode.

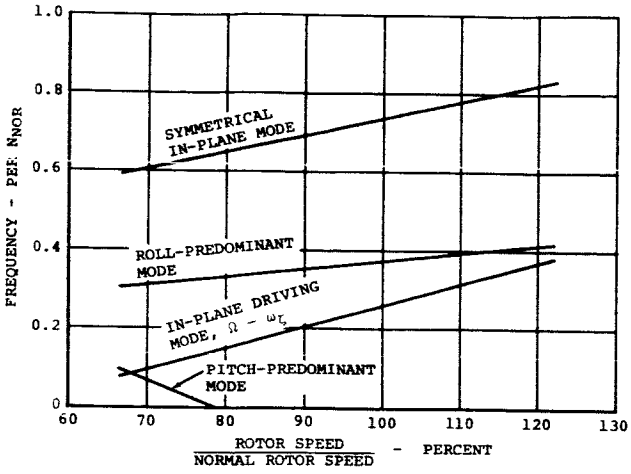

Figure 5. Coupled Resonance Characteristics

Figures 6, 7, and 8 show the time histories of three hover air-resonance points which are at constant collective pitch of 133 percent θ_{NOR} (1g hover collective at N_{NOR}) with rotor speeds of 100 percent, 72 percent, and 67 percent N_{NOR} respectively. At N_{NOR} the chord bending decayed after the excitation terminated, at a rate of approximately 1 percent of critical damping, and the body participation was barely detectable. Approaching the stability boundary at 72 percent rpm, the chord bending took longer to decay compared to the 100 percent rpm case. Body participation was quite pronounced in both pitch and roll. While the filtered chord-bending gage in the rotating system was indicating at the blade lag natural frequency, ω_ζ, the body pitch and roll motions responding in the same air-resonance mode were at the fixed-system frequency of $\Omega-\omega_\zeta$. It is of interest that these $\Omega-\omega_\zeta$ body motions are superimposed on some very low-frequency, flying-quality-type motions.

At 67 percent rpm, Figure 8, the air-resonance mode started to diverge after being excited; when the body was snubbed, the blade motion decayed and returned to the 1/rev forced response.

The response characteristics described here held true for all airspeeds tested up to a scaled test speed limit of 225 knots.

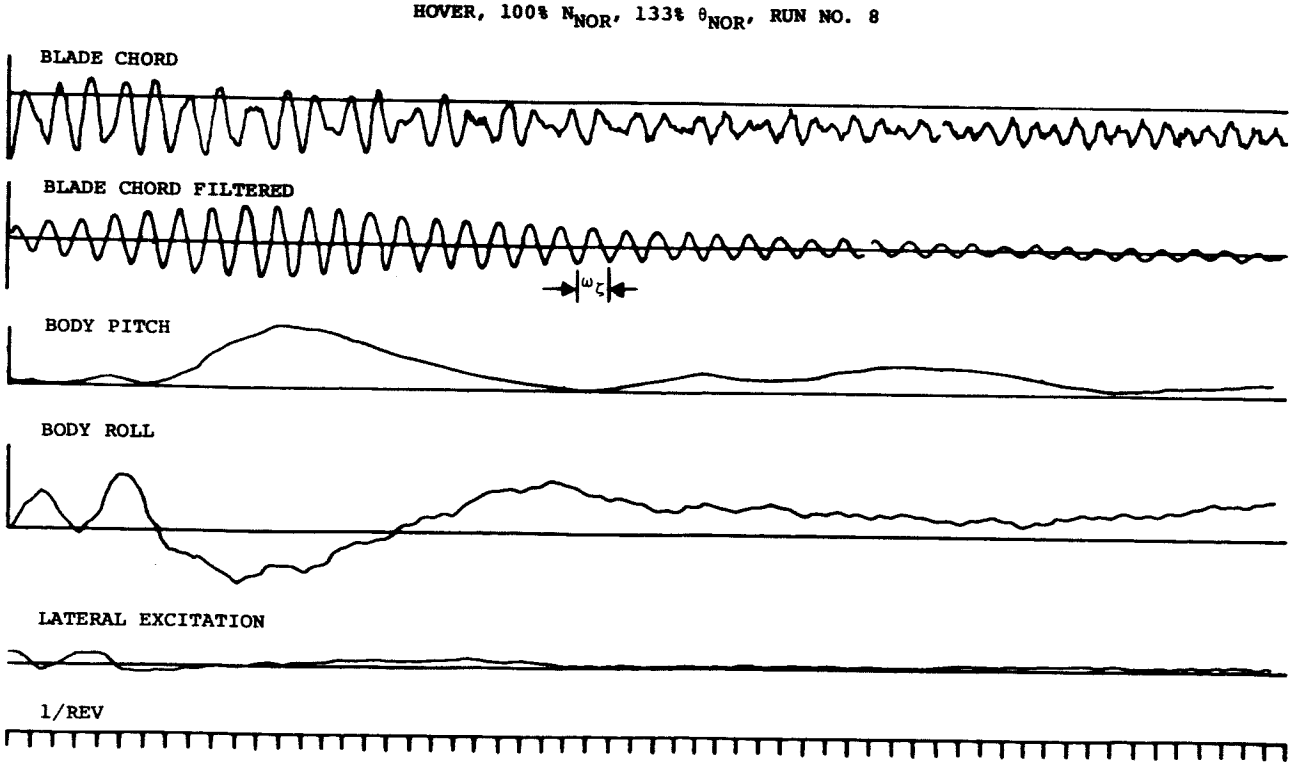

Figure 6. Response Time Histories in Hover at N_{NOR}

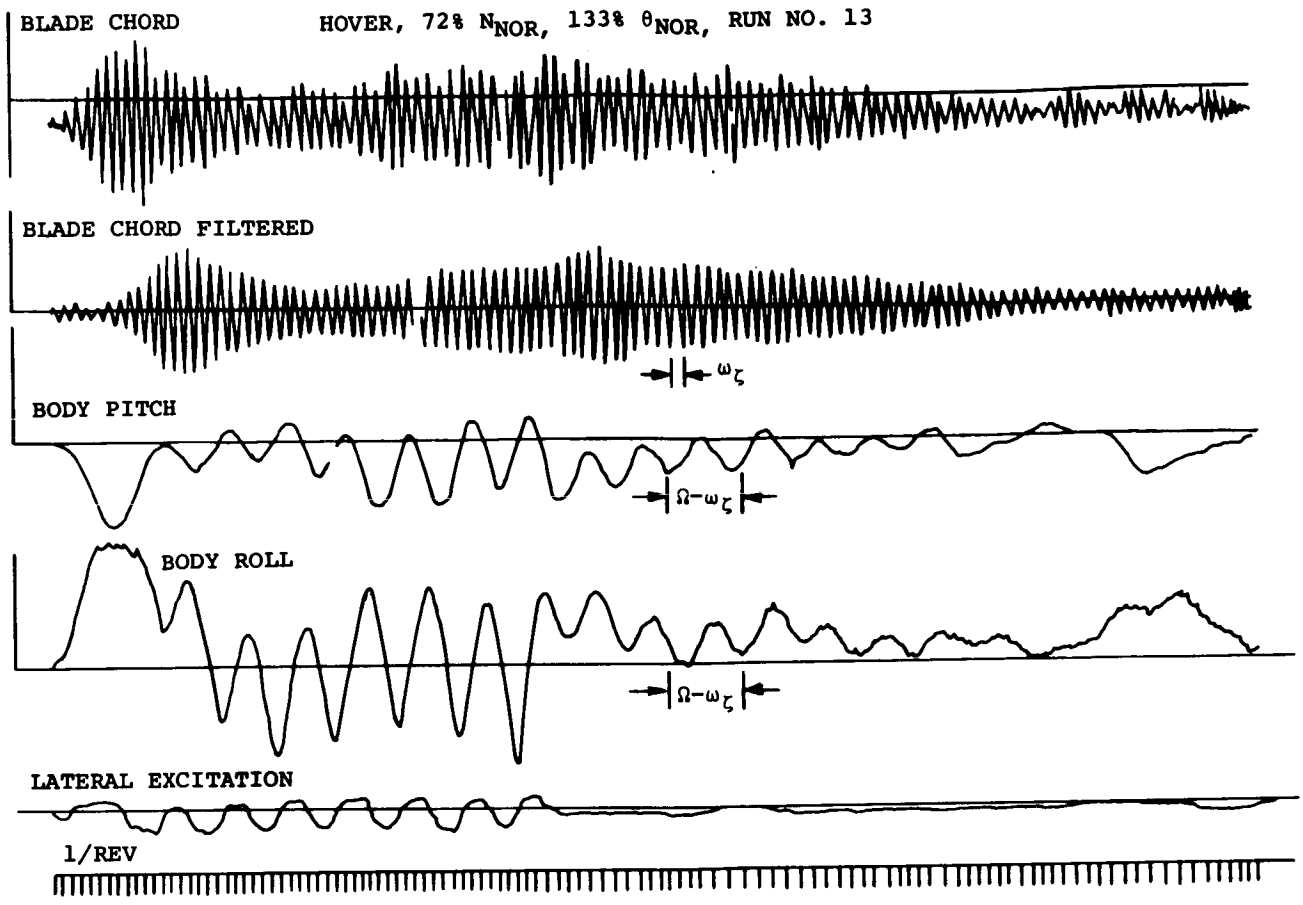

Figure 7. Response Time Histories in Hover at 72 Percent N_{NOR}

Analytical Model

To treat the dynamically and aerodynamically coupled rotor-airframe air-resonance problem, the analytical model shown in Figure 9 is used. In this model, the elastic cantilevered blade is represented by a spring-restrained, hinged rigid blade. Three hinges are used to simulate the first flap, first lag, and first torsion modes, in that order from inboard to outboard. In addition, a pitch degree of freedom is provided inboard of the flap hinge to facilitate the simulation of any torsional stiffness distribution relative to the flap and lag hinges. The blade model includes built-in pitch axis precone, blade sweep, kinematic pitch-flap and pitch-lag coupling, and a variable chordwise center-of-gravity distribution over the blade span.

The aerodynamic model is based on current blade-element theory and can handle all hover, forward flight, and maneuver flight conditions. It uses two-dimensional airfoil data with stall, reverse-flow, and compressibility effects.

The airframe has five rigid-body freedoms: longitudinal, lateral, vertical, pitch, and roll; and two flexible freedoms: pylon pitch and pylon roll. The equations of motion are nonlinear and are solved by a numerical time-history solution technique. The blade degrees of freedom are calculated for each individual blade.

To evaluate the aeroelastic stability, the aircraft can be perturbed from the trimmed state. For air-resonance investigations this is usually done by oscillatory stick excitations, which can be simulated in any frequency. The time history of each degree of freedom is then subjected to an oscillation analysis program to obtain the frequencies, amplitudes, phases, and damping coefficients. A more detailed discussion of this analytical procedure can be found in Reference 2.

Using a linear lift-curve slope, this coupled analysis in hover can be reduced to a set of second-order differential equations with constant coefficients by applying the quasi-normal coordinate transformation

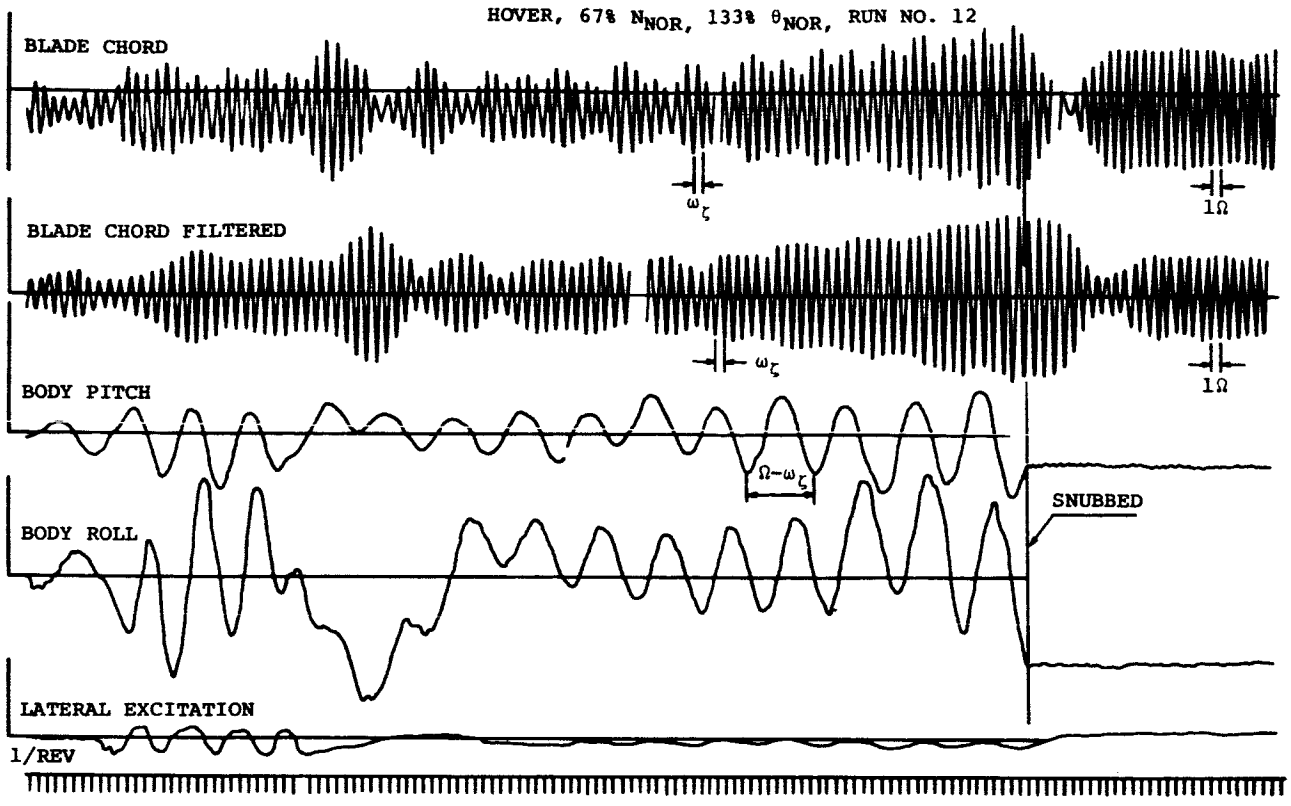

Figure 8. Response Time Histories in Hover at 67 Percent N_{NOR}

for the rotating coordinates[3]. This enables the closed-form solution. The eigenvalues and eigenvectors thus obtained yield the information on frequencies, damping, and mode shapes.

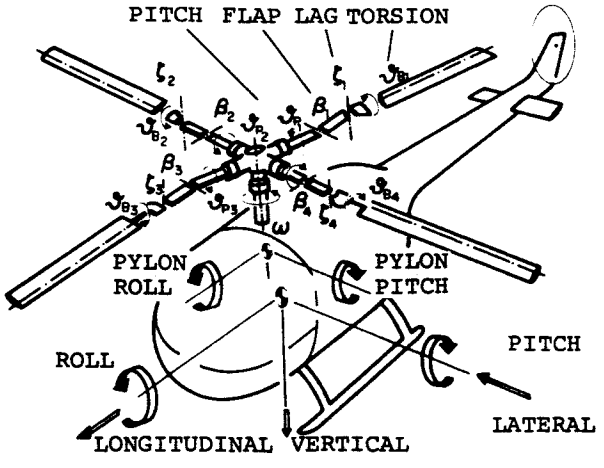

Figure 9. Coupled Rotor-Fuselage Analytical Model

Correlation

Rotor Thrust

Figure 10 shows the air-resonance mode modal damping ratio variations with thrust at N_{NOR} in hover. The agreement between test and analysis is quite good. The propitious trend with increasing collective pitch is due partly to the increase of aerodynamic damping, but is mainly a result of the favorable pitch-flap-lag coupling. A typical blade elastic coupling is shown in Figure 18 where the blade flap, lag, and pitch torsion responses to a cyclic-pitch input are indicated. The type of elastic coupling of this rotor system is discussed in more detail in a subsequent section.

Rotor Speed

Shown in Figure 11 are the test correlations of the air-resonance mode damping variation with rotor speed at constant collective pitch (133 percent θ_{NOR}) in hover. The analytical results are in good agreement with test points over the whole rotor speed range. The stability boundary corresponding to the resonance with the body-pitch-predominant mode at low rpm is predicted well by theory. The somewhat higher level of damping of the test points might indicate that the structural damping of the real model blade is higher than the 0.5 percent damping assumed in the analysis.

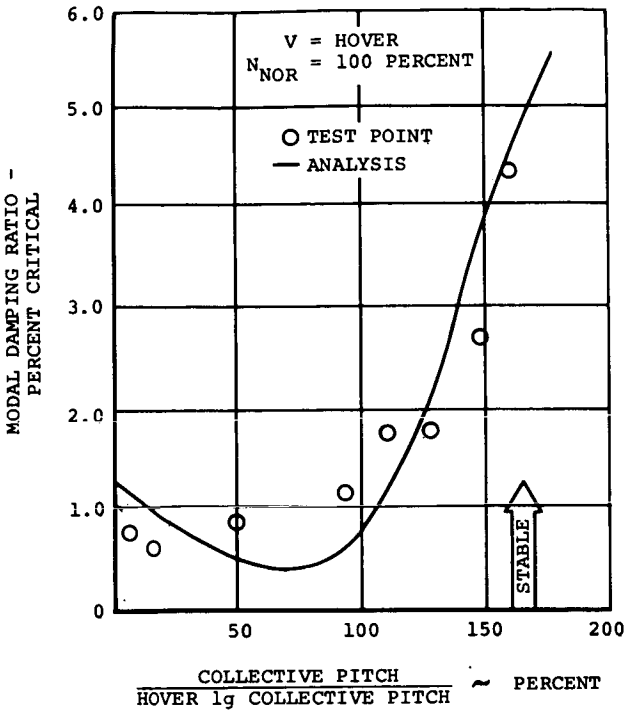

Figure 10. Effect of Thrust on Air-Resonance Stability

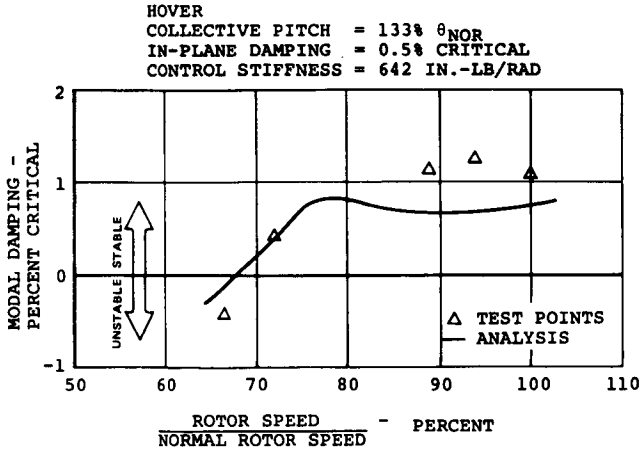

Figure 11. Effect of Rotor Speed on Air-Resonance Stability

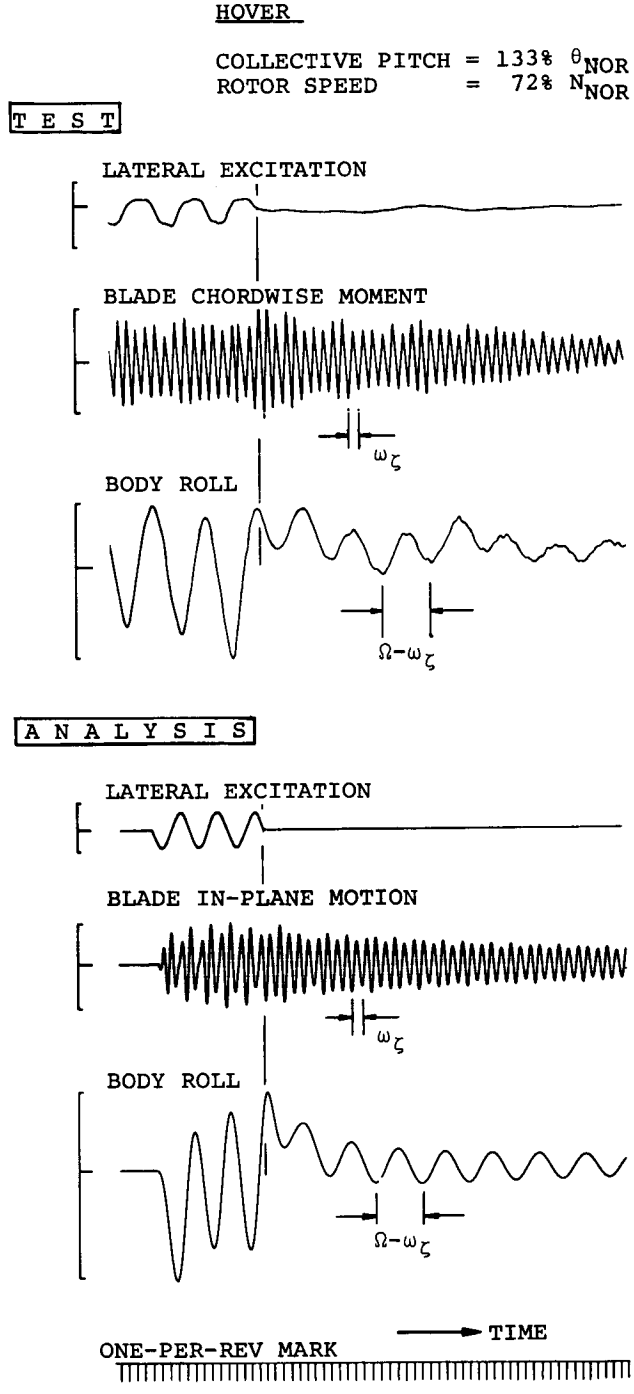

Figure 12. Correlation of Test and Analysis of Time Histories in Hover

The good agreement of Figure 11 is merely a reflection of the excellent correlation between test and analysis in the time-history waveform of blade and body motions. One example is shown in Figure 12. For this case the oscillation analysis program yields a damping coefficient of 0.39 percent at blade lag natural frequency for the rotating blade.

Forward Flight

The test trend of air-resonance mode damping with airspeed is also verified by analysis in Figure 13. Test points shown in this diagram were obtained with constant collective pitch, so that they do not correspond to a 1g-thrust/level-flight condition. The analysis was

performed under the same collective/shaft-angle settings to get an exact simulation of the test conditions. At 150 knots, the collective pitch is slightly reduced, from 133 percent to 111 percent, which produces a sharp decrease in rotor thrust. Therefore the air-resonance mode is less stable than for a normal 1g-thrust condition.

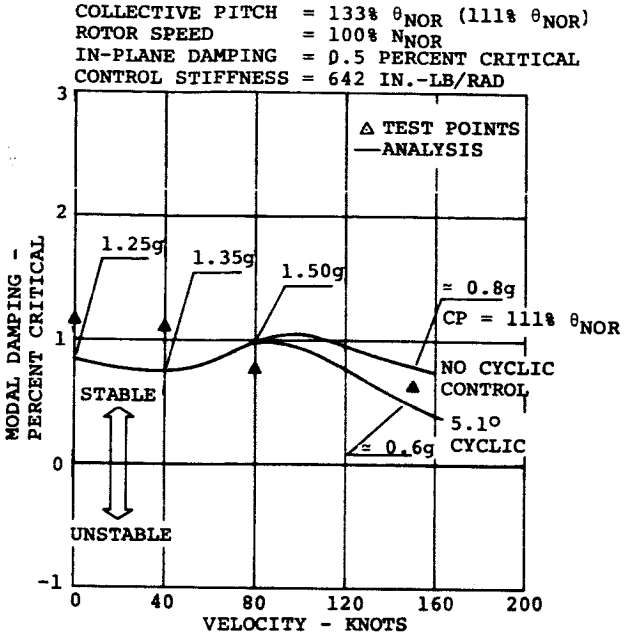

Figure 13. Effect of Forward Speed on Air-Resonance Stability at Constant Collective Pitch

Theory shows some influence of cyclic control on air-resonance stability at high speed. As longitudinal cyclic also controls rotor thrust in forward flight, this variation of air-resonance stability comes solely from the change in rotor thrust. With thrust held constant the stability is insensitive to steady 1/rev cyclic-pitch variation. This is shown in a later section.

In Figure 14 one example of a typical time history at a scaled airspeed of 80 knots is compared between test and analysis. When one considers the complex frequency modulations during this excited air-resonance case, the correlation can be said to be excellent. This should indicate that theory allows a definitive and reliable view of a helicopter's stability characteristics.

Additional test results of air-resonance stability in forward flight are illustrated in Figure 15. This trend, which was obtained for a 1g/level-flight condition, follows the rotor power curve quite well. As shown in Figure 10, for a moderate range of thrust variation, say around 1g, the air-resonance mode becomes more stable with increasing thrust and less stable with decreasing thrust. The forward-speed trend here simply reflects this thrust (and aerodynamic coning angle) dependency. This trend, which shows that the air-resonance mode stability improves significantly at high forward speeds, is also apparent in the BO-105 flight test data[2].

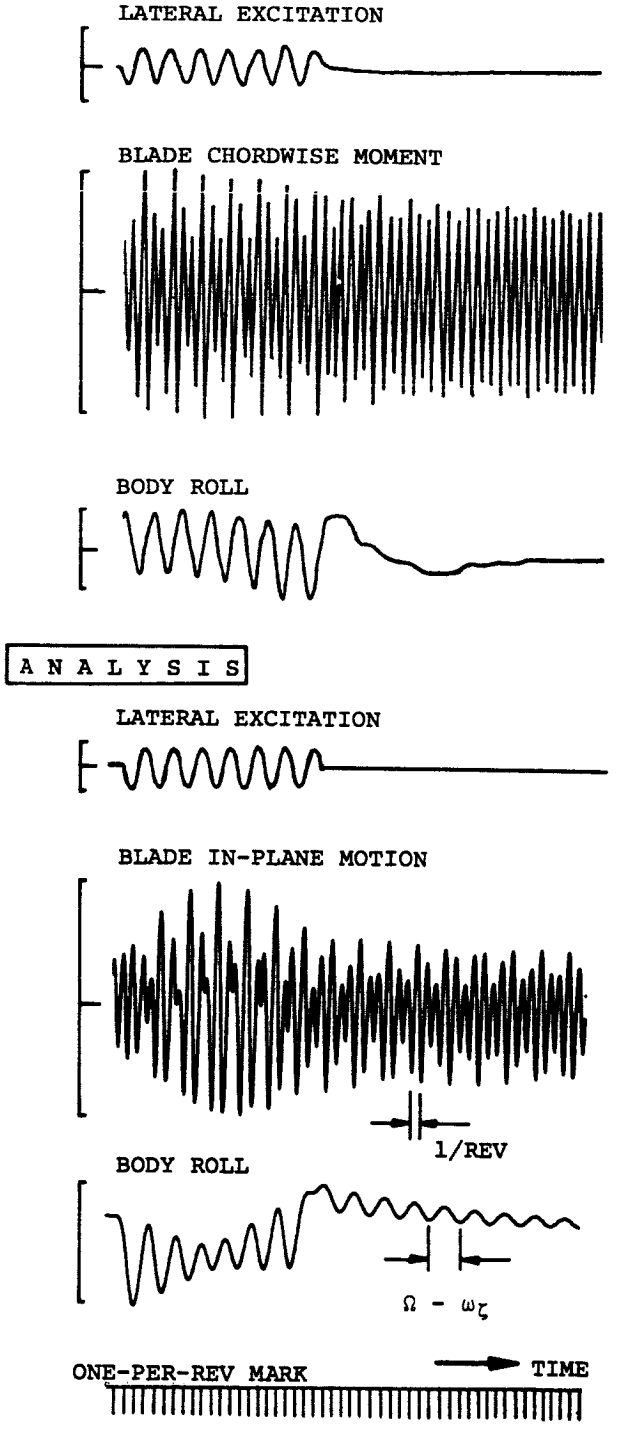

Figure 14. Correlation of Test and Analysis of Time Histories in Forward Flight

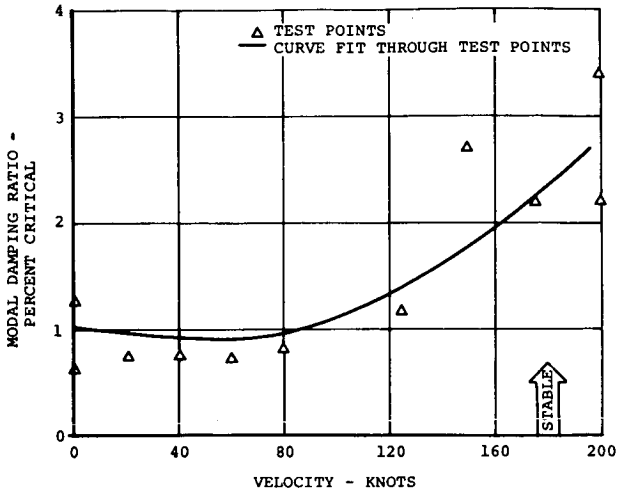

Figure 15. Effect of Forward Speed on Air-Resonance Stability in 1g Level Flight

Physics of Air Resonance

General

The mechanism and the stability characteristics of air resonance have been well described in numerous papers.[1,2,4,5,6] It suffices to say here that the soft-in-plane hingeless-rotor system derives its inherent stability mainly from the powerful flap damping. While rotors with untwisted blades may have substantial reduction in the flap damping near zero thrust, the damping available remains essentially unchanged for blades with nominal twist. Figure 16 shows the test data for various blades of different twist. Above a thrust coefficient of 0.005, the twisted blade and the untwisted blade both have the same thrust-per-collective slope. While the untwisted blade has a drastic reduction in slope with reduction in thrust in both theory and test, that of the twisted blade remains the same.

Let us examine the coupling terms that are inherent in the hingeless rotor system with an equivalent hinge sequence of pitch-flap-lag from inboard to outboard. One term that stands out is the perturbation pitch moment produced by the induced drag (steady force) acting through a moment arm of vertical-flapping displacement (perturbation deflection). This flap-pitch coupling term due to the induced drag has the sense of flap up/pitch noseup. Figure 17 compares the air-resonance mode damping of the same rotor system with this particular coupling term suppressed. With the induced-drag term suppressed, the air-resonance mode does not become unstable at high collective where the induced drag dominates.

By the same consideration, the air-resonance mode should become more stable in descent since during descent, the induced drag acts toward the leading edge producing a flap-pitch coupling of flap-up/pitch-nose-down sense, which is stabilizing.

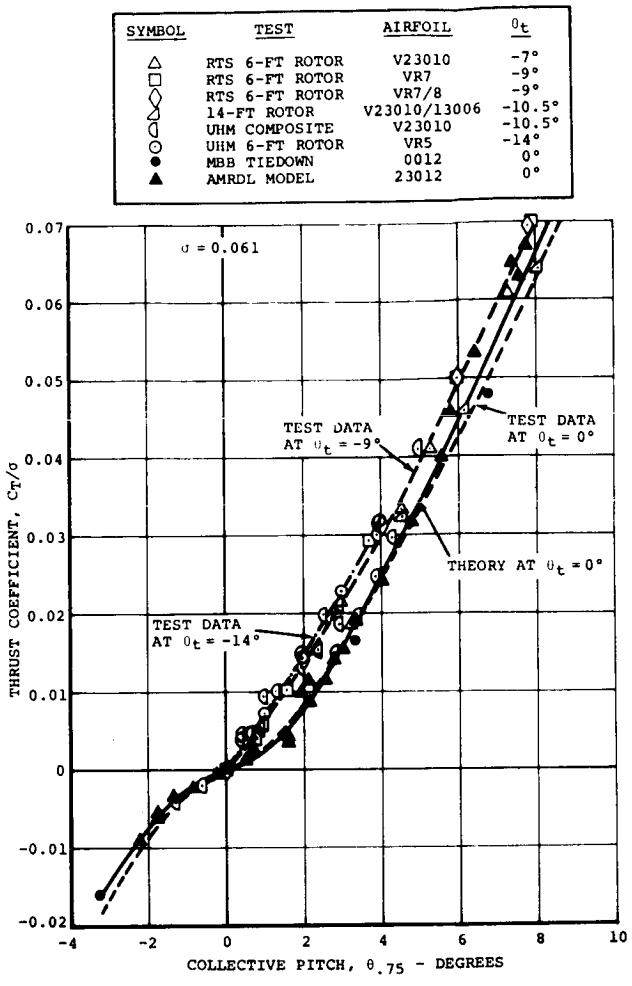

Figure 16. Effect of Blade Twist on Thrust Coefficient

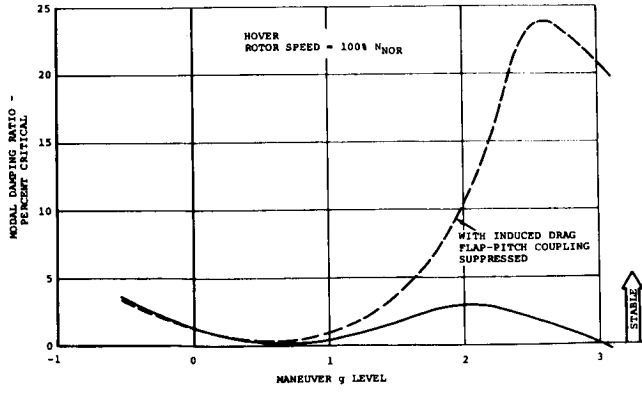

Figure 17. Stability Characteristics With Suppression of Flap-Pitch Coupling Term Due to Induced Drag

Pitch-Flap-Lag Coupling Characteristics

For a complete understanding of the elastic-coupling characteristics of a hingeless rotor with a pitch-flap-lag sequence of hinges, all blade motions must be considered together. For this purpose it is instructive to analyze a simple cyclic-pitch case in hover. In Figure 18 the elastic flap, lead-lag, and pitch motions are shown over one rotor revolution. It can be seen clearly that the flap and lag motions are accompanied by an elastic pitch torsion, the resultant coupling being in the sense of flap up/lead forward/pitch nosedown. For a clear understanding this complex coupling can be divided into two distinct coupling phenomena: the one equivalent to a negative pitch-flap coupling (flap up/pitch nosedown), the other equivalent to a positive pitch-lag coupling (lead forward/pitch nosedown). The coupling factors are 0.4 degree pitch per degree flap and 0.6 degree pitch per degree lag.

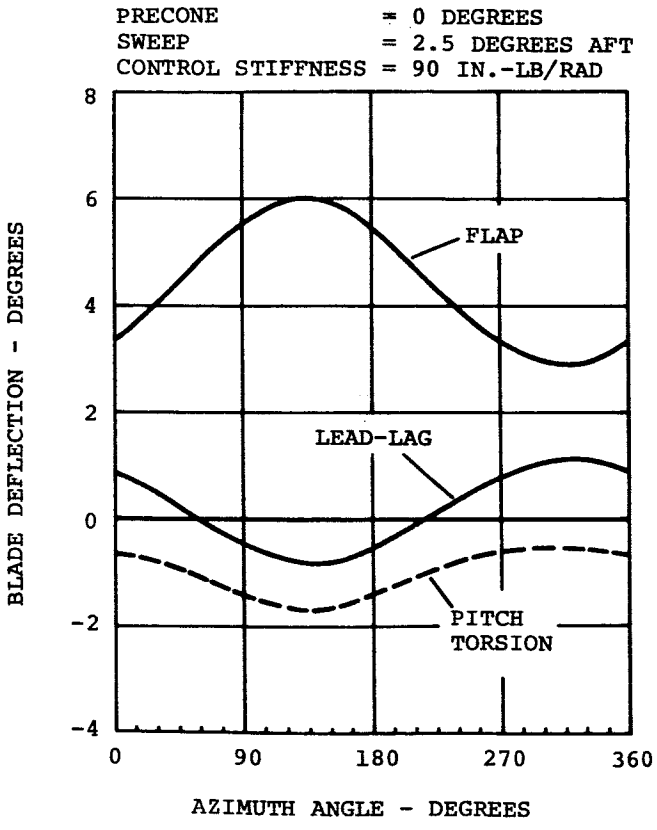

Figure 18. Blade Elastic Coupling

Besides the well-known stabilizing effect of pitch-flap coupling, the pitch-lag part of the total coupling is of utmost importance for the in-plane motions of the blade. Positive pitch-lag coupling (decrease of pitch as the blade leads forward, increase of pitch as the blade lags back) has a highly stabilizing effect on the lead-lag oscillations. Recent investigations[1,2] have shown that these coupling characteristics can be influenced by several hub and blade parameters, for example, by feathering axis precone, blade sweep, and control system flexibility. Some of these design rules have already been applied to this model rotor design (low precone, aft sweep, soft control systems).

Parametric Sensitivities

The following paragraphs describe the air-resonance mode stability sensitivities obtained from the model test.

Climb and Descent

Figure 19 shows the sensitivity with 1g climb and descent at a scaled airspeed of 80 knots. With normal control system stiffness (90 in.-lb/rad), descent stabilizes the mode as discussed in the previous section; conversely, climb has a destabilizing effect.

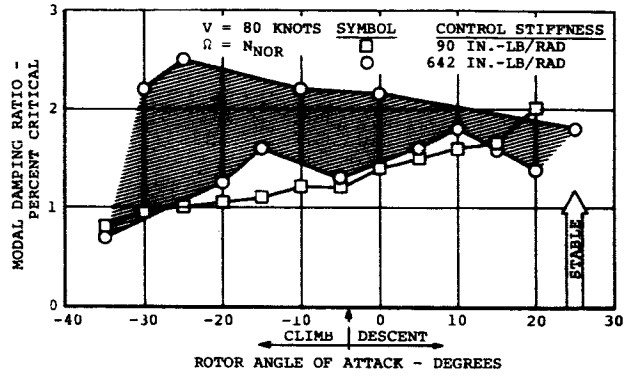

Figure 19. Effects of Climb, Descent, and Control System Stiffness on Air-Resonance Stability

Control System Stiffness

Also shown in Figure 19 are the test data obtained with the control system stiffness seven times stiffer than normal. The effect of climb and descent almost disappeared. Since the stability is affected by the pitch-flap-lag coupling, a stiff control system minimizes the coupling effect, be it favorable or unfavorable.

Precone

Precone of the pitch axis directly alters the pitch-flap-lag coupling. The beneficial effect of lower precone has been evaluated many times.[1,2,7] Figure 20 shows the test confirmation of the favorable effect of the low precone.

Cyclic Trim

An evaluation of the cyclic trim on the air-resonance stability was accomplished by varying the angle of incidence of the tail. The tail incidence angle was varied from 2 degrees through 45 degrees. As shown in Figure 21, the stability is insensitive to the range of cyclic-trim variation at constant thrust. This suggests that the steady 1/rev cyclic-pitch variation in forward flight can be ignored with respect to the air resonance.

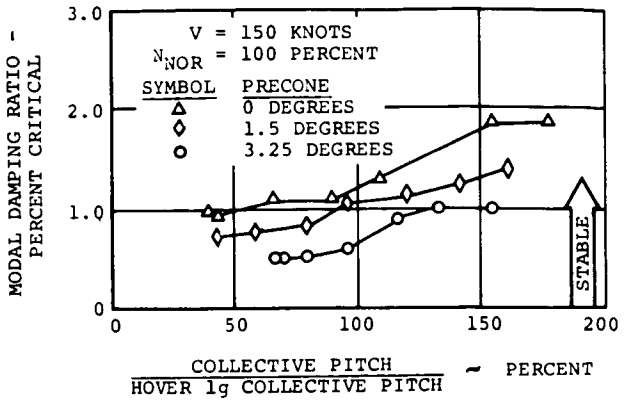

Figure 20. Effect of Blade Precone on Air-Resonance Stability

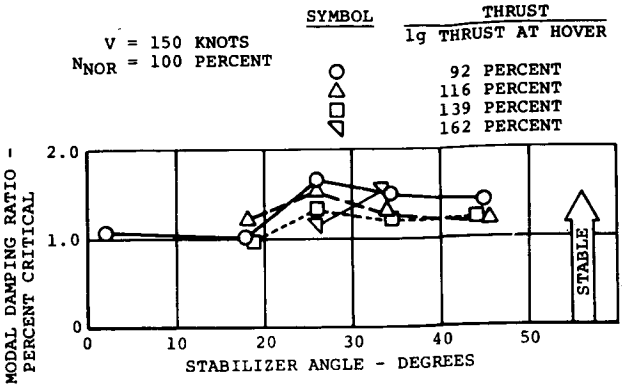

Figure 21. Effect of the Incidence Angle of the Horizontal Tail on Air-Resonance Stability

Conclusions

1. The air-resonance mode stability is sensitive to collective pitch (thrust).

2. Air-resonance mode stability is also sensitive to climb and descent; that is, descent is stabilizing while climb is destabilizing.

3. The prime coupling term in the rotor system which causes the degradation of stability at high thrust is the induced drag. This coupling also provides the trend versus climb and descent.

4. Air-resonance mode stability in 1g level flight shows the rotor-power-curve trend with highly stable characteristics at high speed.

5. The elastic-coupling behavior of the model rotor with normal control system stiffness is characterized by a pitch-flap coupling (0.4 degree pitch per degree flap) and a pitch-lag coupling (0.6 degree pitch per degree lag).

6. High control system stiffness minimizes the flap-pitch coupling effectiveness and reduces the sensitivity of the air-resonance stability to design parameters which are otherwise influential.

7. Less precone is stabilizing for a soft-in-plane hingeless-rotor system with an equivalent hinge sequence of pitch-flap-lag from inboard to outboard.

8. Variation in cyclic trim does not affect air-resonance stability.

9. The testing technique to define air-resonance modal damping discretely at many operational conditions proved highly successful. Use of these methods to define modal damping, rather than defining only the boundaries, allows for a more definitive view of an aircraft's stability characteristics.

References

1. Burkam, J.E., and Miao, W., EXPLORATION OF AEROELASTIC STABILITY BOUNDARIES WITH A SOFT-IN-PLANE HINGELESS-ROTOR MODEL, Preprint No. 610, 28th Annual National Forum of the American Helicopter Society, Washington, D.C., May 1972.

2. Huber, H.B., EFFECT OF TORSION-FLAP-LAG COUPLING ON HINGELESS ROTOR STABILITY, Preprint No. 731, 29th Annual National Forum of the American Helicopter Society, Washington, D.C., May 1973.

3. Gabel, R., and Capurso, V., EXACT MECHANICAL INSTABILITY BOUNDARIES AS DETERMINED FROM THE COLEMAN EQUATION, Journal of the American Helicopter Society, January 1962.

4. Lytwyn, R.T., Miao, W., and Woitsch, W., AIRBORNE AND GROUND RESONANCE OF HINGELESS ROTORS, Preprint No. 414, 26th Annual National Forum of the American Helicopter Society, Washington, D.C., June 1970.

5. Donham, R.E., Cardinale, S.V., and Sachs, I.B., GROUND AND AIR RESONANCE CHARACTERISTICS OF A SOFT INPLANE RIGID ROTOR SYSTEM, Journal of the American Helicopter Society, October 1969.

6. Woitsch, W., and Weiss, H., DYNAMIC BEHAVIOR OF A HINGELESS FIBERGLASS ROTOR, AIAA/AHS VTOL Research, Design, and Operations Meeting, Atlanta, Georgia, February 1969.

7. Hodges, D.H., and Ormiston, R.A., STABILITY OF ELASTIC BENDING AND TORSION OF UNIFORM CANTILEVERED ROTOR BLADES IN HOVER, AIAA/ASME/SAE 14th Structures, Structural Dynamics, and Materials Conference, Williamsburg, Virginia, March 1973.